Combining Bayesian active learning and stratified sampling for bounding small failure probability under hybrid uncertainties

X. Y. Zhu[1)], Y. F. Cui[1)] and P. F. Wei[1)]
[1)]*School of Power and Energy, Northwestern Polytechnical University*
Xi'an 710072, China, zhuxinyu@mail.nwpu.edu.cn

Abstract: Forward uncertainty propagation of hybrid uncertainties from inputs to the outputs, and estimating the resultant bounds of failure probability under insufficient information is a critical issue for the safety and reliability assessment. The two curses—namely the double-loop structure and the extremely small failure probability—pose challenges to the numerical efficiency and global convergence of existing methods when solving this problem. The recently developed Collaborative and Adaptive Bayesian Optimization (CABO) has been recognized as an appealing scheme for breaking the double-loop curse. Under this methodology framework, this work presents a novel algorithm, named combining Bayesian active learning and stratified sampling (BAL-SS), for efficiently estimating the bounds of small failure probability. Specifically, a new learning function, with the aim of adaptive balance of exploration and exploitation, is developed for implementing Bayesian optimization during the marginal space of epistemic uncertainty, and then develops a Bayesian quadrature rule that combines active learning and stratified sampling to estimate the target small failure probabilities. The proposed BAL-SS algorithm is devised by collaborative implementation of the above two key procedures, in the marginal supports of epistemic and aleatory uncertainties, to sequentially approach the global optima and estimate the corresponding failure probabilities with desired accuracy. Effectiveness of the proposed method is ultimately demonstrated with numerical benchmark study and practical engineering applications.

Keywords: Hybrid uncertainty propagation; Small failure probability; Bayesian active learning; Stratified sampling; Gaussian process regression.

1. Introduction

Estimating the small failure probability is a critical issue for the safety assessment of critical structures in many engineering fields, such as civil and aerospace engineering. However, the standard mathematical formulation of this problem requires precise probability models of the random input variables. This requirement often renders state-of-the-art developments inapplicable to real-world engineering applications, as precise probability models are generally inaccessible due to a lack of or poor quality of information (Beer, 2013). Under this situation, imprecise probability models, like the probability box (p-box) models (Crespo, 2013), the fuzzy probability models (Stein, 2013; Blair 2001), the evidence theory (Agarwal, 2004; McGill, 2008) and the hierarchical probability models (Zhang, 2018) have been developed. These frameworks are all capable of separately modeling the two types of uncertainties owning to the hierarchical model structures, but also bring a great challenge for propagating the uncertainties, which is the so-called "double-loop curse". This challenge becomes even more severe when estimating the bounds of extremely small failure probabilities, a common requirement in structural reliability analysis.

In case of hybrid uncertainties, some attempts have been presented for addressing the double-loop curse challenge. The standard implementation follows a double-loop structure: the outer loop performs probabilistic analysis with Monte Carlo simulation (MCS) over aleatory variables, while the inner loop conducts an interval analysis for each realization to determine the bounds of the model response by using either intrusive method like interval finite element analysis or non-intrusive method like particle swarm optimization (PSO). This approach, known as interval Monte Carlo Simulation (IMCS), is intrusive due to its reliance on repeated interval finite element analyses (Zhang, 2010; Zhang, 2013; Zhao, 2024). Building upon this double-loop algorithm and aiming for greater efficiency, the interval importance sampling method represents a significant improvement (Zhang, 2012; Alvarez, 2018). While the double-loop method is conceptually simple and arguably requires less subjective information, it remains difficult to directly incorporate the effect of interval parameters into structural reliability assessments, as it necessitates evaluating the families of all candidate probability distributions within the interval bounds.

To break the nested loops, single-loop methods have been extensively developed, including Extended Monte Carlo Simulation (EMCS) (Wei, 2014), Non-intrusive Imprecise Stochastic Simulation (NISS) (Wei, 2019; Wei, 2019; Song 2020), the operator norm method (Faes, 2021), and Collaborative and Adaptive Bayesian Optimization (CABO) (Hong, 2024; Hong, 2023; Wei, 2021). The implementation of single-loop methods for resolving double-loop problems primarily follows two strategic directions: decoupling the nested procedural structure and adopting non-intrusive computational techniques. The former strategy addresses the inherent randomness of the input by discretizing any random fields or processes into a finite set of random variables. This is typically achieved through methods such as the expansion optimal linear estimation (EOLE) (Li, 1993), Karhunen–Loève (KL) expansion (Huang, 2007), stochastic Harmonic function representation (SHFR) (Chen, 2017), or sparse Gaussian process (GP) based on simulation (Wilson, 2020; Vakili, 2021). While this discretization is a essential prerequisite for decoupling, it can itself introduce a significant computational burden. The latter strategy, employing non-intrusive techniques, leverages the model as a black box, requiring only input-output evaluations without the need for surrogate modeling of the limit state function. This approach offers great flexibility. However, a key limitation arises when dealing with high-dimensional epistemic inputs, as the estimation of bounds for model response moments and failure probabilities can become inefficient or intractable.

The task of this work is to extend our previous work CABO (Wei, 2021) for estimating the bounds of failure probability functions under hybrid uncertainties. In this work, we propose a novel reliability analysis framework, named Bayesian active learning with stratified sampling (BAL-SS), designed for efficiently bounding failure probability with hybrid uncertainties. By strategically integrating an improved Upper Confidence Bound (UCB) learning function, BAL-SS is designed to efficiently overcome high-dimensional bottlenecks and precisely bound failure probabilities with complex hybrid uncertainties.

2. Problem Statement

Define $\boldsymbol{y} = g(\boldsymbol{x})$ as the limit state function (LSF) and $\boldsymbol{y}$ refers to the univariate model output. The uncertainty in $\boldsymbol{y}$ originates from the uncertainty $\boldsymbol{x}$. In this paper, we consider the case that the input variables are characterized by three types of uncertainty characteristic models, which are referred to as the $[\boldsymbol{x}_{\mathrm{I}}, \boldsymbol{x}_{\mathrm{II}}, \boldsymbol{x}_{\mathrm{III}}]$ hereinafter. Let $\boldsymbol{x}_{\mathrm{I}} = [\boldsymbol{x}_{\mathrm{I}}^1, \boldsymbol{x}_{\mathrm{I}}^2, ..., \boldsymbol{x}_{\mathrm{I}}^{n_{\mathrm{I}}}]^{\mathrm{T}}$ represent n_{I}-dimensional random variables with aleatory uncertainty, characterized by a precise probability density function (PDF) $f_{\mathrm{I}}(\boldsymbol{x}_{\mathrm{I}})$. Then define $\boldsymbol{x}_{\mathrm{II}} = [\boldsymbol{x}_{\mathrm{II}}^1, \boldsymbol{x}_{\mathrm{II}}^2, ..., \boldsymbol{x}_{\mathrm{II}}^{n_{\mathrm{II}}}]^{\mathrm{T}}$ as a n_{II} -dimensional random variables incorporating both aleatory uncertainty and epistemic uncertainty, represented by the p-box model $f_{\mathrm{II}}(\boldsymbol{x}_{\mathrm{II}}|\boldsymbol{\theta})$. The epistemic uncertainty of $\boldsymbol{x}_{\mathrm{II}}$ is associated with the non-deterministic distribution parameters $\boldsymbol{\theta}$, which are characterized by hyper-rectangular $[\boldsymbol{\theta}^{\mathrm{L}},\boldsymbol{\theta}^{\mathrm{U}}]$. Finally, let $\boldsymbol{x}_{\mathrm{III}}=[\boldsymbol{x}_{\mathrm{III}}^{1},\boldsymbol{x}_{\mathrm{III}}^{2},...,\boldsymbol{x}_{\mathrm{III}}^{n_{\mathrm{III}}}]^{\mathrm{T}}$ denote n_{III}-dimensional random variables with epistemic uncertainty quantified by the hyper-rectangular $[\boldsymbol{x}_{\mathrm{III}}^{\mathrm{L}},\boldsymbol{x}_{\mathrm{III}}^{\mathrm{U}}]$. Assuming all these three types of inputs are independent, and the joint PDF of $\boldsymbol{x}_{\mathrm{I}}$ and $\boldsymbol{x}_{\mathrm{II}}$ can be formulated as $f_{\mathrm{I}}(\boldsymbol{x}_{\mathrm{I}})=\prod_{i=1}^{n_{\mathrm{I}}}f_{\mathrm{I}}^{i}(x_{\mathrm{I}}^{i})$ and $f_{\mathrm{II}}(\boldsymbol{x}_{\mathrm{II}}|\boldsymbol{\theta})=\prod_{i=1}^{n_{\mathrm{II}}}f_{\mathrm{II}}^{i}(x_{\mathrm{II}}^{i}|\theta^{i})$. In summary, the aleatory uncertainties are derived from $\boldsymbol{x}_{\mathrm{I}}$ and $\boldsymbol{x}_{\mathrm{II}}$ with PDF of $f_{\mathrm{I}}(\boldsymbol{x}_{\mathrm{I}})$ and $f_{\mathrm{II}}(\boldsymbol{x}_{\mathrm{II}}|\boldsymbol{\theta})$, and the epistemic uncertainties are derived from deterministic interval variables $\boldsymbol{x}_{\mathrm{III}}$ and $\boldsymbol{\theta}$. For reliability analysis, assume $\boldsymbol{y}<0$ means structure failure and failure domain is denoted as $F=\{(\boldsymbol{x}_{\mathrm{I}},\boldsymbol{x}_{\mathrm{II}},\boldsymbol{x}_{\mathrm{III}}):g(\boldsymbol{x}_{\mathrm{I}},\boldsymbol{x}_{\mathrm{II}},\boldsymbol{x}_{\mathrm{III}})<0\}$. The indicate function $I_F(\boldsymbol{x}_{\mathrm{I}},\boldsymbol{x}_{\mathrm{II}},\boldsymbol{x}_{\mathrm{III}})$ of failure domain is defined as $I_F(\boldsymbol{x}_{\mathrm{I}},\boldsymbol{x}_{\mathrm{II}},\boldsymbol{x}_{\mathrm{III}})=1$ when $(\boldsymbol{x}_{\mathrm{I}},\boldsymbol{x}_{\mathrm{II}},\boldsymbol{x}_{\mathrm{III}})\in F$ and $I_F(\boldsymbol{x}_{\mathrm{I}},\boldsymbol{x}_{\mathrm{II}},\boldsymbol{x}_{\mathrm{III}})=0$ when $(\boldsymbol{x}_{\mathrm{I}},\boldsymbol{x}_{\mathrm{II}},\boldsymbol{x}_{\mathrm{III}})\notin F$. Based on the above settings, the failure probability is estimated by integrating out aleatory parameters $\boldsymbol{x}_{\mathrm{I}}$ and $\boldsymbol{x}_{\mathrm{II}}$:

$$P_f(\boldsymbol{x}_{\mathrm{III}},\boldsymbol{\theta})=\int_{R^{n_{\mathrm{I}}+n_{\mathrm{II}}}}I_F(\boldsymbol{x}_{\mathrm{I}},\boldsymbol{x}_{\mathrm{II}},\boldsymbol{x}_{\mathrm{III}},\boldsymbol{\theta})f(\boldsymbol{x}_{\mathrm{I}})f_{\mathrm{II}}(\boldsymbol{x}_{\mathrm{II}}|\boldsymbol{\theta})d\boldsymbol{x}_{\mathrm{I}}d\boldsymbol{x}_{\mathrm{II}}. \tag{1}$$

The main objective of this work is to quantify the bounds of the failure probability parameterized by epistemic uncertainty variables. The lower bound and upper bound of failure probability are separately defined as:

$$P_{f,\mathrm{L}}=\min_{\boldsymbol{x}_{\mathrm{III}}\in[\boldsymbol{x}_{\mathrm{III}}^{\mathrm{L}},\boldsymbol{x}_{\mathrm{III}}^{\mathrm{U}}],\boldsymbol{\theta}\in[\boldsymbol{\theta}^{\mathrm{L}},\boldsymbol{\theta}^{\mathrm{U}}]}P_f(\boldsymbol{x}_{\mathrm{III}},\boldsymbol{\theta}), \tag{2a}$$

$$P_{f,\mathrm{U}}=\max_{\boldsymbol{x}_{\mathrm{III}}\in[\boldsymbol{x}_{\mathrm{III}}^{\mathrm{L}},\boldsymbol{x}_{\mathrm{III}}^{\mathrm{U}}],\boldsymbol{\theta}\in[\boldsymbol{\theta}^{\mathrm{L}},\boldsymbol{\theta}^{\mathrm{U}}]}P_f(\boldsymbol{x}_{\mathrm{III}},\boldsymbol{\theta}). \tag{2b}$$

It is seen that Eqs.(2a) and (2b) involve a double-loop structure. In the inner-loop, aleatory uncertainties are addressed and Bayesian integration is performed to estimate the failure probability, where the propagation of the aleatory uncertainty has to be conducted for each realization during the search for epistemic parameters. While in the outer-loop, Bayesian optimization is performed to search for the global optima.

3. Bayesian active learning with stratified sampling for bounding failure probability

3.1. Gaussian Process Regression

Before reporting the main procedure of Bayesian integration, the isoprobabilistic transformation is used to decouple $\boldsymbol{x}_{\mathrm{II}}$, as $\boldsymbol{x}_{\mathrm{II}}$ represent the variable with the mixture of epistemic uncertainty and aleatory uncertainty. Assume $F_{\mathrm{II}}(\boldsymbol{x}_{\mathrm{II}}|\boldsymbol{\theta})$ denotes the cumulative distribution function (CDF) of $\boldsymbol{x}_{\mathrm{II}}$. It is known that CDF of any variable follows a uniform distribution in interval [0,1]. Let $\boldsymbol{u}=(u^1,u^2,...,u^{n_{\mathrm{II}}})$ with each element being independent of each other and let $u^i=F_{\mathrm{II}}^{i}(x_{\mathrm{II}}^{i}|\theta^i)$, the inverse transformation can be expressed as $x_{\mathrm{II}}^{i}=F_{\mathrm{II}}^{i\,-1}(u^i|\theta^i)$. Then the LSF with arguments $\boldsymbol{\omega}=(\boldsymbol{x}_{\mathrm{I}},\boldsymbol{u},\boldsymbol{x}_{\mathrm{III}},\boldsymbol{\theta})$ is denoted by $\boldsymbol{y}=g(\boldsymbol{\omega})$. After that, it is required to transform $\boldsymbol{x}_{\mathrm{I}}$ and $\boldsymbol{u}$ into variables with normal standard distribution.

Assume $g(\boldsymbol{\omega})$ is characterized by a Gaussian distribution, represented as $\hat{g}(\boldsymbol{\omega})\sim\mathcal{GP}(m(\boldsymbol{\omega}),\kappa(\boldsymbol{\omega},\boldsymbol{\omega}'))$, where $\boldsymbol{\omega}=[\boldsymbol{x}_{\mathrm{I}},\boldsymbol{u},\boldsymbol{x}_{\mathrm{III}},\boldsymbol{\theta}]$. $m(\boldsymbol{\omega})$ is the prior mean function, which can be set as 0, constant and polynomial.

$\boldsymbol{\kappa}(\boldsymbol{\omega},\boldsymbol{\omega}')$ is prior covariance and can measure the prior covariance of correlation $g(\boldsymbol{\omega})$ at site $\boldsymbol{\omega}$ and site $\boldsymbol{\omega}'$. Here the square kernel function serves as the covariance kernel function, and is formulated as:

$$\boldsymbol{\kappa}(\boldsymbol{\omega},\boldsymbol{\omega}')=\sigma_0^2\exp\left(-\frac{1}{2}(\boldsymbol{\omega}-\boldsymbol{\omega}')\varSigma^{-1}(\boldsymbol{\omega}-\boldsymbol{\omega}')^{\mathrm{T}}\right), \tag{3}$$

where σ_0^2 and $\varSigma$ are hyper parameters of covariance function.

Then define the N_0 -dimension training data vector $\boldsymbol{D}=(\boldsymbol{W},\boldsymbol{Y})$, where $\boldsymbol{W}=[\boldsymbol{\omega}_1;\boldsymbol{\omega}_2;...;\boldsymbol{\omega}_{N_0}]$ are the randomly generated training sample points and $\boldsymbol{Y}=\hat{\mathcal{G}}(\boldsymbol{W})$. The likelihood function is defined as the joint probability density function of Gaussian random vectors, formulated as:

$$\mathcal{L}(\boldsymbol{D})=\frac{1}{(2\pi)^{\frac{N_0}{2}}|\boldsymbol{K}|^{\frac{1}{2}}}\exp\left(-\frac{1}{2}(\boldsymbol{Y}-m(\boldsymbol{W}))^{\mathrm{T}}\boldsymbol{K}^{-1}(\boldsymbol{Y}-m(\boldsymbol{W}))\right), \tag{4}$$

where $\boldsymbol{K}=\boldsymbol{\kappa}(\boldsymbol{W},\boldsymbol{W})$ is the covariance matrix of $\boldsymbol{\omega}$.

The posterior distribution of the prediction $\hat{g}(\boldsymbol{\omega})$ at $\boldsymbol{\omega}$ is estimated with the hyper parameters of Gaussian process. The posterior distribution can be represented as $\hat{g}(\boldsymbol{\omega})\sim\mathcal{GP}(\mu_g(\boldsymbol{\omega}),\mathrm{cov}_g(\boldsymbol{\omega},\boldsymbol{\omega}'))$, where $\mu_g(\boldsymbol{\omega})$ is the posterior mean function of $\hat{g}(\boldsymbol{\omega})$. The variance σ_g^2 and posterior covariance $\mathrm{cov}_g(\boldsymbol{\omega},\boldsymbol{\omega}')$ are indicated as:

$$\mu_g(\boldsymbol{\omega})=m(\boldsymbol{\omega})+\boldsymbol{\kappa}(\boldsymbol{W},\boldsymbol{\omega})^{\mathrm{T}}\boldsymbol{K}^{-1}(Y-m(\boldsymbol{W})), \tag{5}$$

$$\sigma_g^2(\boldsymbol{\omega})=\sigma_0^2-\boldsymbol{\kappa}(\boldsymbol{W},\boldsymbol{\omega})^{\mathrm{T}}\boldsymbol{K}^{-1}\boldsymbol{\kappa}(\boldsymbol{W},\boldsymbol{\omega}), \tag{6}$$

$$\mathrm{cov}_g(\boldsymbol{\omega},\boldsymbol{\omega}')=\boldsymbol{\kappa}(\boldsymbol{\omega},\boldsymbol{\omega}')-\boldsymbol{\kappa}(\boldsymbol{W},\boldsymbol{\omega})^{\mathrm{T}}\boldsymbol{K}^{-1}\boldsymbol{\kappa}(\boldsymbol{W},\boldsymbol{\omega}'), \tag{7}$$

where posterior variance $\sigma_g^2(\boldsymbol{\omega})=\mathrm{cov}_g(\boldsymbol{\omega},\boldsymbol{\omega})$ and measures the prediction error at $\boldsymbol{\omega}$ based on posterior GPR model.

Once the GPR model is trained, the induced failure probability function follows a random process with unknown distribution parameters as failure probability function defined in Eq.(1) is not a linear map of LSF $g(\boldsymbol{x}_{\mathrm{I}},\boldsymbol{u},\boldsymbol{x}_{\mathrm{III}},\boldsymbol{\theta})$. The bounds of prediction based on posterior GPR model, denoted as $\mu_g^{\mathrm{L}}(\boldsymbol{x}_{\mathrm{I}},\boldsymbol{u},\boldsymbol{x}_{\mathrm{III}},\boldsymbol{\theta})$ and $\mu_g^{\mathrm{U}}(\boldsymbol{x}_{\mathrm{I}},\boldsymbol{u},\boldsymbol{x}_{\mathrm{III}},\boldsymbol{\theta})$ are then defined by incorporating the posterior standard deviation as a measure of epistemic uncertainty. Let a be a scaling factor that quantifies the uncertainty magnitude, the bounds of prediction can be expressed as:

$$\mu_g^{\mathrm{U}}(\boldsymbol{x}_{\mathrm{I}},\boldsymbol{u},\boldsymbol{x}_{\mathrm{III}},\boldsymbol{\theta})=\mu_g(\boldsymbol{x}_{\mathrm{I}},\boldsymbol{u},\boldsymbol{x}_{\mathrm{III}},\boldsymbol{\theta})+a\sigma_g(\boldsymbol{x}_{\mathrm{I}},\boldsymbol{u},\boldsymbol{x}_{\mathrm{III}},\boldsymbol{\theta}), \tag{8a}$$

$$\mu_g^{\mathrm{L}}(\boldsymbol{x}_{\mathrm{I}},\boldsymbol{u},\boldsymbol{x}_{\mathrm{III}},\boldsymbol{\theta})=\mu_g(\boldsymbol{x}_{\mathrm{I}},\boldsymbol{u},\boldsymbol{x}_{\mathrm{III}},\boldsymbol{\theta})-a\sigma_g(\boldsymbol{x}_{\mathrm{I}},\boldsymbol{u},\boldsymbol{x}_{\mathrm{III}},\boldsymbol{\theta}), \tag{8b}$$

where a is a constant parameter and typically set to $a=1$ by default.

Then the bounds of failure probability $\overline{P}_f(a,\boldsymbol{x}_{\mathrm{III}},\boldsymbol{\theta})$ and $\underline{P}_f(a,\boldsymbol{x}_{\mathrm{III}},\boldsymbol{\theta})$ are formulated as Eq.(9), and the failure probability function is negatively correlated with prediction of GPR model.

$$\begin{aligned}\overline{P}_f(a,\boldsymbol{x}_{\mathrm{III}},\boldsymbol{\theta})&=\Pr(\mu_g(\boldsymbol{X}_{\mathrm{I}},\boldsymbol{U},\boldsymbol{x}_{\mathrm{III}},\boldsymbol{\theta})-a\sigma_g(\boldsymbol{X}_{\mathrm{I}},\boldsymbol{U},\boldsymbol{x}_{\mathrm{III}},\boldsymbol{\theta})<0)\\&=\int I(\mu_g(\boldsymbol{x}_{\mathrm{I}},\boldsymbol{u},\boldsymbol{x}_{\mathrm{III}},\boldsymbol{\theta})-a\sigma_g(\boldsymbol{x}_{\mathrm{I}},\boldsymbol{u},\boldsymbol{x}_{\mathrm{III}},\boldsymbol{\theta})<0)f(\boldsymbol{x}_{\mathrm{I}})f(\boldsymbol{u})d\boldsymbol{x}_{\mathrm{I}}d\boldsymbol{u},\end{aligned} \tag{9a}$$

$$\begin{aligned}\underline{P}_f(a,\boldsymbol{x}_{\mathrm{III}},\boldsymbol{\theta})&=\Pr(\mu_g(\boldsymbol{X}_{\mathrm{I}},\boldsymbol{U},\boldsymbol{x}_{\mathrm{III}},\boldsymbol{\theta})+a\sigma_g(\boldsymbol{X}_{\mathrm{I}},\boldsymbol{U},\boldsymbol{x}_{\mathrm{III}},\boldsymbol{\theta})<0)\\&=\int I(\mu_g(\boldsymbol{x}_{\mathrm{I}},\boldsymbol{u},\boldsymbol{x}_{\mathrm{III}},\boldsymbol{\theta})+a\sigma_g(\boldsymbol{x}_{\mathrm{I}},\boldsymbol{u},\boldsymbol{x}_{\mathrm{III}},\boldsymbol{\theta})<0)f(\boldsymbol{x}_{\mathrm{I}})f(\boldsymbol{u})d\boldsymbol{x}_{\mathrm{I}}d\boldsymbol{u},\end{aligned} \tag{9b}$$

where $\overline{P}_f(a,\boldsymbol{x}_{\mathrm{III}},\boldsymbol{\theta})$ and $\underline{P}_f(a,\boldsymbol{x}_{\mathrm{III}},\boldsymbol{\theta})$ measure the range of uncertainty of the estimated failure probability function value at the point $(\boldsymbol{x}_{\mathrm{III}},\boldsymbol{\theta})$ based on current GPR model for better optimization in the next steps, $\boldsymbol{X}_{\mathrm{I}}$ and $\boldsymbol{U}$ are MCS sample set of random input $\boldsymbol{x}_{\mathrm{I}}$ and $\boldsymbol{u}$ respectively. Under the epistemic uncertainty generated from GPR model, the true value of the failure probability function lies within the range delimited by the upper and lower bounds.

For characterizing the random process of failure probability function, the posterior mean $\mu_g(\boldsymbol{x}_{\mathrm{I}},\boldsymbol{u},\boldsymbol{x}_{\mathrm{III}},\boldsymbol{\theta})$, and its bounds $\mu_g^{\mathrm{L}}(\boldsymbol{x}_{\mathrm{I}},\boldsymbol{u},\boldsymbol{x}_{\mathrm{III}},\boldsymbol{\theta})$ and $\mu_g^{\mathrm{U}}(\boldsymbol{x}_{\mathrm{I}},\boldsymbol{u},\boldsymbol{x}_{\mathrm{III}},\boldsymbol{\theta})$ are mapped to failure probability function by MCS. In this case, the upper and lower bound of failure probability based on current GPR model can be inferred as follows:

$$\overline{P}_f(a,\boldsymbol{x}_{\mathrm{III}},\boldsymbol{\theta}) = \frac{1}{N}\sum_{j=1}^{N} I\left(\mu_g(\boldsymbol{X}_{\mathrm{I}}^j,\boldsymbol{U}^j,\boldsymbol{x}_{\mathrm{III}},\boldsymbol{\theta}) - a\sigma_g(\boldsymbol{X}_{\mathrm{I}}^j,\boldsymbol{U}^j,\boldsymbol{x}_{\mathrm{III}},\boldsymbol{\theta})\right) \tag{10a}$$

$$\underline{P}_f(a,\boldsymbol{x}_{\mathrm{III}},\boldsymbol{\theta}) = \frac{1}{N}\sum_{j=1}^{N} I\left(\mu_g(\boldsymbol{X}_{\mathrm{I}}^j,\boldsymbol{U}^j,\boldsymbol{x}_{\mathrm{III}},\boldsymbol{\theta}) + a\sigma_g(\boldsymbol{X}_{\mathrm{I}}^j,\boldsymbol{U}^j,\boldsymbol{x}_{\mathrm{III}},\boldsymbol{\theta})\right) \tag{10b}$$

where $\underline{P}_f(a,\boldsymbol{x}_{\mathrm{III}},\boldsymbol{\theta}) \leqslant P_f(a,\boldsymbol{x}_{\mathrm{III}},\boldsymbol{\theta}) \leqslant \overline{P}_f(a,\boldsymbol{x}_{\mathrm{III}},\boldsymbol{\theta})$, and N is the size of sample pool.

3.2. Combination With Stratified Sampling

The MCS method is widely employed for failure probability estimation. However, for reliability analysis involving rare events with a failure probability on the order of 10^{-k}, the required sample set must be at least 10^{k+1} to ensure the statistically significant verification. Such a large sample set will lead to substantial computational cost, especially in the context of Bayesian integration. To overcome this challenge, the stratified sampling (SS) method is adopted, which inherits the advantages of the MCS method while improving its efficiency in estimating failure probability in the rare events.

First, transform the aleatory variable $\boldsymbol{x}_{\mathrm{I}}$ into the standard normal space. Then both $\boldsymbol{x}_{\mathrm{I}}$ and $\boldsymbol{u}$ serve as random inputs within the epistemic uncertainty space. They are combined into a composite vector of random variables $\boldsymbol{z}=[\boldsymbol{x}_{\mathrm{I}},\boldsymbol{u}]$ which jointly follows standard normal distribution. The process begins with a set of initial samples $\boldsymbol{z}=(z_1,z_2,...,z_{n_z})$ with n_z-dimensional independent standard normal variables. Subsequently generate a set of independent samples $\boldsymbol{Z}$ with size of N_z, and divide these samples into s stratified subdomains $(\beta_1^2 \leqslant \|z_1\| \leqslant \beta_2^2, \beta_2^2 \leqslant \|z_2\| \leqslant \beta_3^2, ..., \beta_s^2 \leqslant \|z_s\| \leqslant \beta_{s+1}^2)$ with $\beta_i\,(0=\beta_1<\beta_2<...<\beta_s<\beta_{s+1}=\infty)$. The value of the radius β is chosen with Eq.(11).

$$\beta_i = \sqrt{(\chi_{n_z}^2)^{-1}(1-p_0^i)}, \tag{11}$$

where $\chi_{n_z}^2(\beta_i^2)$ is the CDF of chi-square distribution with n_z degrees of freedom and $(\chi_{n_z}^2)^{-1}$ is the inverse function of $\chi_{n_z}^2(\beta_i^2)$, the value of failure probability parameter p_0 is chosen as 0.1. The probability density function (PDF) of truncated samples in i-th truncated subdomain is expressed as:

$$f_{\boldsymbol{Z}}^{\mathrm{tr}(i)}(\boldsymbol{z}) = \begin{cases} \dfrac{1}{\chi_{n_z}^2(\beta_{i+1}^2) - \chi_{n_z}^2(\beta_i^2)} f_{\boldsymbol{Z}}(\boldsymbol{z}), \text{ if } \beta_i^2 \leqslant \|\boldsymbol{z}_i\|^2 \leqslant \beta_{i+1}^2 \\ 0\,, \text{ otherwise} \end{cases}, \tag{12}$$

where $f_{\boldsymbol{Z}}^{\mathrm{tr}(i)}(\boldsymbol{z})$ satisfy $\int_{\beta_i^2 \leqslant \|z_i\|^2 \leqslant \beta_{i+1}^2} f_{\boldsymbol{Z}}^{\mathrm{tr}(i)}(\boldsymbol{z}) = 1$.

Then define the random inputs $\boldsymbol{z}$ with $\boldsymbol{z} = r \cdot \boldsymbol{\alpha}$, where r and $\boldsymbol{\alpha}$ are the length and direction of $\boldsymbol{z}$ respectively. The direction vector $\boldsymbol{\alpha}$ can be obtained by $\boldsymbol{\alpha}_j = \dfrac{\boldsymbol{z}_j}{\|\boldsymbol{z}_j\|^2}$, while the length vector r^2 satisfies the chi-square distribution with n_z degree of freedom, thus generate N_z samples with:

$$r_j^{(i)} = \sqrt{(\chi_{n_z}^2)^{-1}([\chi_{n_z}^2(\beta_{i+1}^2) - \chi_{n_z}^2(\beta_i^2)] \cdot v_j^{(i)} + \chi_{n_z}^2(\beta_i^2))} \tag{13}$$

where $v_j^{(i)}$ follows uniform distribution of interval [0,1] and $r_j^{(i)}$ represents the length of i-th part of j-th direction of sampling. Then generate samples by using $\boldsymbol{z}_j^{(i)} = r_j^{(i)} \cdot \boldsymbol{\alpha}_j$. Here an example with two-dimensional random inputs is used to illustrate the sampling principle of SS in Figure 1. As is shown in Figure 1, the whole aleatory space is divided into seven parts with β_i and samples in each subdomain are independent of samples in other subdomains.

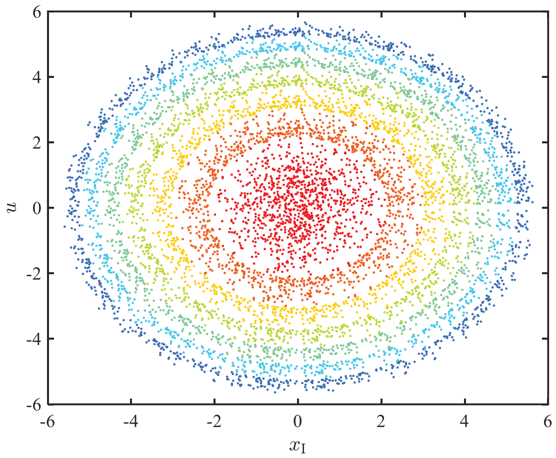

Figure 1. The generated samples of two-dimensional random inputs by SS.

The failure probability of the whole aleatory sphere at fixed $(\boldsymbol{x}_{\mathrm{III}}, \boldsymbol{\theta})$ can be formulated as Eq.(14) through the total probability formula:

$$\begin{aligned} P_f(\boldsymbol{x}_{\mathrm{III}}, \boldsymbol{\theta}) &= \Pr\{g(\boldsymbol{z}, \boldsymbol{x}_{\mathrm{III}}, \boldsymbol{\theta}) \leqslant 0 \,|\, \boldsymbol{z} \in F\} \\ &= \sum_{i=1}^{s} \Pr\{g(\boldsymbol{z}, \boldsymbol{x}_{\mathrm{III}}, \boldsymbol{\theta}) \leqslant 0 \,|\, \beta_i^2 \leqslant \|\boldsymbol{z}_i\|^2 \leqslant \beta_{i+1}^2\} \Pr\{\beta_i^2 \leqslant \|\boldsymbol{z}_i\|^2 \leqslant \beta_{i+1}^2\} \\ &= \sum_{i=1}^{s} \Pr\{g(\boldsymbol{z}, \boldsymbol{x}_{\mathrm{III}}, \boldsymbol{\theta}) \leqslant 0 \,|\, \beta_i^2 \leqslant \|\boldsymbol{z}_i\|^2 \leqslant \beta_{i+1}^2\} [\chi_{n_z}^2(\beta_{i+1}^2) - \chi_{n_z}^2(\beta_i^2)] \end{aligned} \tag{14}$$

where $\|\boldsymbol{z}_i\|^2 = \sum_{j=1}^{n_z} z_{i,j}^2$ denotes the distance between $\boldsymbol{z}_i$ and original point and is distributed as chi-square distribution, $\Pr(\cdot)$ represents the probability of $g(\boldsymbol{z}, \boldsymbol{x}_{\mathrm{III}}, \boldsymbol{\theta}) \leqslant 0$.

The first term in Eq.(14) can be easily obtained by MCS sampling in the sphere:

$$\begin{aligned} P_f^{(i)}(\boldsymbol{x}_{\mathrm{III}},\boldsymbol{\theta}) &= \int I_F(\boldsymbol{z},\boldsymbol{x}_{\mathrm{III}},\boldsymbol{\theta}) f_{\boldsymbol{Z}}^{\mathrm{tr}(i)}(\boldsymbol{z})\,d\boldsymbol{z} \\ &= \frac{1}{N_z}\sum_{j=1}^{N_Z} I_F(\boldsymbol{z}_j^{(i)},\boldsymbol{x}_{\mathrm{III}},\boldsymbol{\theta}) \end{aligned} \tag{15}$$

So based on MCS sampling method, Eq.(14) can be expressed as is shown in Eq.(16):

$$\begin{aligned} P_f(\boldsymbol{x}_{\mathrm{III}},\boldsymbol{\theta}) &= \sum_{i=1}^{s}\{[\chi_{n_z}^2(\beta_{i+1}^2)-\chi_{n_z}^2(\beta_i^2)]P_f^{(i)}(\boldsymbol{x}_{\mathrm{III}},\boldsymbol{\theta})\} \\ &= \sum_{i=1}^{s}\left\{[\chi_{n_z}^2(\beta_{i+1}^2)-\chi_{n_z}^2(\beta_i^2)]\frac{1}{N_z}\sum_{j=1}^{N_z} I_F(\boldsymbol{z}_j^{(i)},\boldsymbol{x}_{\mathrm{III}},\boldsymbol{\theta})\right\} \end{aligned} \tag{16}$$

Calculate the expectation on both sides of Eq.(16):

$$\begin{aligned} E[P_f(\boldsymbol{x}_{\mathrm{III}},\boldsymbol{\theta})] &= E\left\{\sum_{i=1}^{s}\left[[\chi_{n_z}^2(\beta_i^2)-\chi_{n_z}^2(\beta_{i+1}^2)]\cdot\frac{1}{N_z}\sum_{j=1}^{N_z} I_F(\boldsymbol{z}_j^{(i)},\boldsymbol{x}_{\mathrm{III}},\boldsymbol{\theta})\right]\right\} \\ &= \sum_{i=1}^{s}\left\{[\chi_{n_z}^2(\beta_i^2)-\chi_{n_z}^2(\beta_{i+1}^2)]\cdot E\left[\frac{1}{N_z}\sum_{j=1}^{N_z} I_F(\boldsymbol{z}_j^{(i)},\boldsymbol{x}_{\mathrm{III}},\boldsymbol{\theta})\right]\right\} \\ &= P_f \end{aligned} \tag{17}$$

The estimation of failure probability based on stratified beta-sphere sampling technique is unbiased which is equal to the expectation. Then calculate the variance on both sides of the Eq.(16):

$$\mathrm{Var}[P_f(\boldsymbol{x}_{\mathrm{III}},\boldsymbol{\theta})] = \sum_{i=1}^{s}\left[[\chi_{n_z}^2(\beta_{i+1}^2)-\chi_{n_z}^2(\beta_i^2)]^2\cdot\frac{[P_f^{(i)}(\boldsymbol{x}_{\mathrm{III}},\boldsymbol{\theta})-(P_f^{(i)}(\boldsymbol{x}_{\mathrm{III}},\boldsymbol{\theta}))^2]}{N_z}\right]. \tag{18}$$

And the COV of this method can be achieved by Eq.(19):

$$\mathrm{COV}[P_f(\boldsymbol{x}_{\mathrm{III}},\boldsymbol{\theta})] = \frac{\sqrt{\mathrm{Var}[P_f(\boldsymbol{x}_{\mathrm{III}},\boldsymbol{\theta})]}}{P_f(\boldsymbol{x}_{\mathrm{III}},\boldsymbol{\theta})}. \tag{19}$$

Based on above assumptions, the expectation and variance are the functions of failure probability estimation, which inherit the accuracy of MCS. The failure probability within each subdomain can be evaluated in parallel, therefore reduces time consumption and improves computational efficiency.

Thus, the failure probability bounds are obtained as shown in Eq.(20) using the general framework defined in Eqs.(10a) and (10b).

$$\overline{P}_f(a,\boldsymbol{x}_{\mathrm{III}},\boldsymbol{\theta}) = \sum_{i=1}^{s}\left\{[\chi_{n_z}^2(\beta_{i+1}^2)-\chi_{n_z}^2(\beta_i^2)]\cdot\left[\frac{1}{N_z}\sum_{j=1}^{N_z} I_F(\mu_g(\boldsymbol{Z}^j,\boldsymbol{x}_{\mathrm{III}},\boldsymbol{\theta})-a\cdot\sigma_g(\boldsymbol{Z}^j,\boldsymbol{x}_{\mathrm{III}},\boldsymbol{\theta}))\right]\right\}, \tag{20a}$$

$$\underline{P}_f(a,\boldsymbol{x}_{\mathrm{III}},\boldsymbol{\theta}) = \sum_{i=1}^{s}\left\{[\chi_{n_z}^2(\beta_{i+1}^2)-\chi_{n_z}^2(\beta_i^2)]\cdot\left[\frac{1}{N_z}\sum_{j=1}^{N_z} I_F(\mu_g(\boldsymbol{Z}^j,\boldsymbol{x}_{\mathrm{III}},\boldsymbol{\theta})+a\cdot\sigma_g(\boldsymbol{Z}^j,\boldsymbol{x}_{\mathrm{III}},\boldsymbol{\theta}))\right]\right\}. \tag{20b}$$

3.3. Bayesian Optimization In Epistemic Uncertainty Space

The SS method is integrated with the GPR model and active learning strategy: the aleatory uncertainty space is first divided into multiple subdomains from which a sample pool is generated. The GPR model is then trained with initial training samples selected from sample pool. With all the above information settled, the

UCB function of Bayesian optimization for maximizing or minimizing the objective $P_f(a,\boldsymbol{x}_{\mathrm{III}},\boldsymbol{\theta})$ can be formulated as:

$$\mathcal{L}_{P_{f,\mathrm{L}}}(a,b,\boldsymbol{x}_{\mathrm{III}},\boldsymbol{\theta})=P_f(a,\boldsymbol{x}_{\mathrm{III}},\boldsymbol{\theta})-b\left(\overline{P}_f(a,\boldsymbol{x}_{\mathrm{III}},\boldsymbol{\theta})-\underline{P}_f(a,\boldsymbol{x}_{\mathrm{III}},\boldsymbol{\theta})\right), \tag{21a}$$

$$\mathcal{L}_{P_{f,\mathrm{U}}}(a,b,\boldsymbol{x}_{\mathrm{III}},\boldsymbol{\theta})=P_f(a,\boldsymbol{x}_{\mathrm{III}},\boldsymbol{\theta})+b\left(\overline{P}_f(a,\boldsymbol{x}_{\mathrm{III}},\boldsymbol{\theta})-\underline{P}_f(a,\boldsymbol{x}_{\mathrm{III}},\boldsymbol{\theta})\right), \tag{21b}$$

where coefficient b scales the predicted covariance of the failure probability estimated by the GPR model $\hat{g}(\boldsymbol{x}_{\mathrm{I}},\boldsymbol{x}_{\mathrm{II}},\boldsymbol{x}_{\mathrm{III}},\boldsymbol{\theta})$. This parameter b governs the trade-off between exploration and exploitation during the Bayesian optimization process.

By setting the learning functions as objective functions which are presented in Eqs.(22a) and (22b), the particle swarm optimization (PSO) method is suggested to search the point with highest or lowest value of learning functions straightforwardly.

$$(\boldsymbol{x}_{\mathrm{III}}^{+},\boldsymbol{\theta}^{+})=\arg\min_{\boldsymbol{x}_{\mathrm{III}}\in[\boldsymbol{x}_{\mathrm{III}}^{\mathrm{L}},\boldsymbol{x}_{\mathrm{III}}^{\mathrm{U}}],\boldsymbol{\theta}\in[\boldsymbol{\theta}^{\mathrm{L}},\boldsymbol{\theta}^{\mathrm{U}}]}\mathcal{L}_{P_{f,\mathrm{L}}}(a,b,\boldsymbol{x}_{\mathrm{III}},\boldsymbol{\theta}), \tag{22a}$$

$$(\boldsymbol{x}_{\mathrm{III}}^{+},\boldsymbol{\theta}^{+})=\arg\max_{\boldsymbol{x}_{\mathrm{III}}\in[\boldsymbol{x}_{\mathrm{III}}^{\mathrm{L}},\boldsymbol{x}_{\mathrm{III}}^{\mathrm{U}}],\boldsymbol{\theta}\in[\boldsymbol{\theta}^{\mathrm{L}},\boldsymbol{\theta}^{\mathrm{U}}]}\mathcal{L}_{P_{f,\mathrm{U}}}(a,b,\boldsymbol{x}_{\mathrm{III}},\boldsymbol{\theta}). \tag{22b}$$

If the values of learning functions $\mathcal{L}_{P_{f,\mathrm{U}}}(a,b,\boldsymbol{x}_{\mathrm{III}},\boldsymbol{\theta})$ and $\mathcal{L}_{P_{f,\mathrm{L}}}(a,b,\boldsymbol{x}_{\mathrm{III}},\boldsymbol{\theta})$ tend to converge, the values of the learning functions of next added point $[\boldsymbol{x}_{\mathrm{III}}^{+},\boldsymbol{\theta}^{+}]$ will be equal to that of the current optimal point $[\boldsymbol{x}_{\mathrm{III}}^{*},\boldsymbol{\theta}^{*}]$. And the search of outer-loop will end till the convergence criteria in Eqs.(23a) and (23b) are satisfied.

$$\frac{|\mathcal{L}_{P_{f,\mathrm{L}}}(a,b,\boldsymbol{x}_{\mathrm{III}}^{+},\boldsymbol{\theta}^{+})-\mathcal{L}_{P_{f,\mathrm{L}}}(a,b,\boldsymbol{x}_{\mathrm{III}}^{*},\boldsymbol{\theta}^{*})|}{|\mathcal{L}_{P_{f,\mathrm{L}}}(a,b,\boldsymbol{x}_{\mathrm{III}}^{*},\boldsymbol{\theta}^{*})|}\leqslant\varepsilon, \tag{23a}$$

$$\frac{|\mathcal{L}_{P_{f,\mathrm{U}}}(a,b,\boldsymbol{x}_{\mathrm{III}}^{+},\boldsymbol{\theta}^{+})-\mathcal{L}_{P_{f,\mathrm{U}}}(a,b,\boldsymbol{x}_{\mathrm{III}}^{*},\boldsymbol{\theta}^{*})|}{|\mathcal{L}_{P_{f,\mathrm{U}}}(a,b,\boldsymbol{x}_{\mathrm{III}}^{*},\boldsymbol{\theta}^{*})|}\leqslant\varepsilon \tag{23b}$$

where ε is a user-defined error tolerance. The value of the error tolerance is governed by the required precision for locating the maxima and minima, and typically falls within the range of 10^{-3} to 10^{-2}.

3.4. Bayesian Integration In Aleatory Uncertainty Space

Once the current best guess $(\boldsymbol{x}_{\mathrm{III}},\boldsymbol{\theta})$ is estimated by solving Eq.(23), it is required to estimate the failure probability at fixed $(\boldsymbol{x}_{\mathrm{III}},\boldsymbol{\theta})$. Based on the principle of MCS, the sign judgment of the probability is vital for failure probability estimation. To improve the accuracy of the GPR surrogate model in characterizing LSF, the points with a high potential risk of nearing the predicted LSF are added to the training process to update the GPR model and then evaluate the failure probability of LSF. These points mainly contain three characteristics: to be with high distribution density because it has high variance and aleatory uncertainty, to be close to LSF with high risk of misjudgment or both at the same time. Currently, the most widely used learning functions are U function (Echard, 2011), expected feasibility function (Bichon, 2008) and H function (Lv, 2015). The U function is applied to this work for its performance on the variance of posterior GPR model and the distance between the predicted and actual LSF value. U function is presented as:

$$U(\boldsymbol{x}_{\mathrm{I}},\boldsymbol{u})=\frac{|\mu_g(\boldsymbol{x}_{\mathrm{I}},\boldsymbol{u},\boldsymbol{x}_{\mathrm{III}}^{+},\boldsymbol{\theta}^{+})|}{\sigma_g(\boldsymbol{x}_{\mathrm{I}},\boldsymbol{u},\boldsymbol{x}_{\mathrm{III}}^{+},\boldsymbol{\theta}^{+})}, \tag{24}$$

and the CDF of the U function $\Phi(U(\boldsymbol{x}_{\mathrm{I}},\boldsymbol{u}))$ is used to represent the probability of making a mistake on the sign of $\hat{g}(\boldsymbol{x}_{\mathrm{I}},\boldsymbol{u},\boldsymbol{x}_{\mathrm{III}},\boldsymbol{\theta})$ at fixed $(\boldsymbol{x}_{\mathrm{III}}^{+},\boldsymbol{\theta}^{+})$. Adding the point and the response of LSF with minimum value of $U(\boldsymbol{x}_{\mathrm{I}},\boldsymbol{u})$ to the training process, the aleatory uncertainty of failure probability based on posterior GPR model will be reduced, which is formulated as:

$$(\boldsymbol{x}_{\mathrm{I}}^{+},\boldsymbol{u}^{+})=\arg\min_{\boldsymbol{x}_{\mathrm{I}}\in\boldsymbol{X}_{\mathrm{I}},\boldsymbol{u}\in\boldsymbol{U}}[U(\boldsymbol{x}_{\mathrm{I}},\boldsymbol{u})]. \tag{25}$$

And the stopping condition is set as $\min(U(\boldsymbol{x}_{\mathrm{I}},\boldsymbol{u}))\geqslant 2$ for $(\boldsymbol{x}_{\mathrm{I}},\boldsymbol{u})\in(\boldsymbol{X}_{\mathrm{I}},\boldsymbol{U})$. The U function equal to 2 corresponds to a probability of misjudging on the sign of $\Phi(-2)=0.023$. As is mentioned in Ref[43], such a stopping criterion guarantees the accuracy of GPR model. In the inner-loop of Bayesian integration in aleatory uncertainty space, U function is used to make GPR model more reliable under current best guess $(\boldsymbol{x}_{\mathrm{III}}{}^{+},\boldsymbol{\theta}^{+})$ by adding the pair $(\boldsymbol{x}_{\mathrm{I}}^{+},\boldsymbol{u}^{+})$. In the outer-loop of Bayesian optimization in epistemic uncertainty space, newly developed learning function is used to search for the bounds of failure probability with minimum or maximum value of $\mathcal{L}_{P_{f,\mathrm{L}}}(a,b,\boldsymbol{x}_{\mathrm{III}},\boldsymbol{\theta})$ and $\mathcal{L}_{P_{f,\mathrm{U}}}(a,b,\boldsymbol{x}_{\mathrm{III}},\boldsymbol{\theta})$. Then the double-loop procedure will end until the convergence criteria for two learning functions are both satisfied.

3.5. SUMMARY OF THE PROPOSED BAL-SS

As we introduced in subsection 3.1, 3.2, 3.3 and 3.4, the aim of this subsection is to present the details for computational process. The basic framework is illustrated in Figure 2.

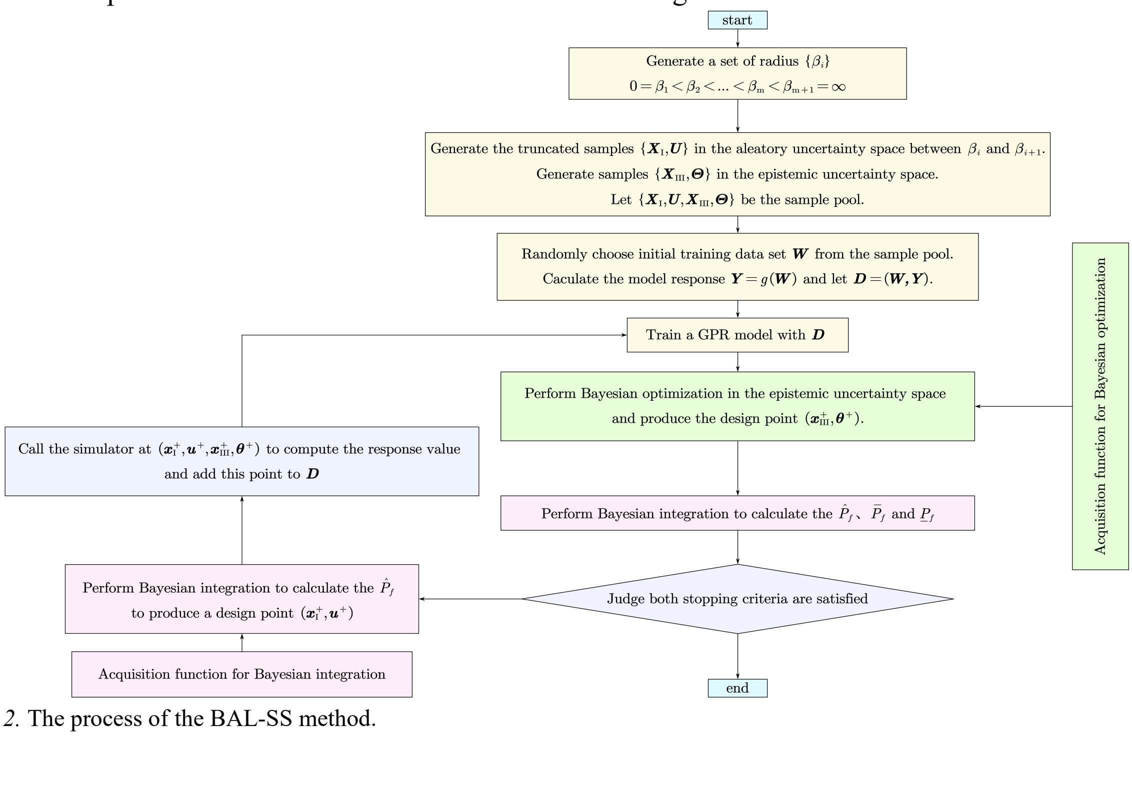

Figure 2. The process of the BAL-SS method.

Firstly, generate a training data set $\boldsymbol{D}$ in the augmented aleatory uncertainty space and epistemic uncertainty space. Train a GPR model with initial training samples. Then solve the outer-loop optimization by Bayesian optimization in the epistemic uncertainty to search for the bounds of failure probability. Solve the inner-loop integral by Bayesian integration to reduce the aleatory uncertainty. In the Bayesian optimization process, developed learning functions are utilized to create the design point $(\boldsymbol{x}_{\mathrm{III}}{}^{+},\boldsymbol{\theta}^{+})$. In the Bayesian integration process, U function is applied to generate the experiment design point $(\boldsymbol{x}_{\mathrm{I}}{}^{+},\boldsymbol{u}^{+})$ and accelerate the convergence process. At last, with newly added point $(\boldsymbol{x}_{\mathrm{I}}{}^{+},\boldsymbol{u}^{+},\boldsymbol{x}_{\mathrm{III}}{}^{+},\boldsymbol{\theta}^{+})$ in the joint probability space, the algorithm will end when both optimization and integration satisfy convergence criteria, which have been reported respectively in subsection 3.3 and 3.4. And the global optimization points will be achieved. Based on different selections of the learning function, the corresponding upper and lower bound of the failure probability can be achieved respectively.

4. Benchmark Studies

4.1. A Three-Dimensional Numerical Example

We consider three-dimensional numerical examples:

$$g_1(x) = 7 - (x_1 + x_3)^2 + x_2 \tag{26}$$

and

$$g_2(x) = 20 - (x_1 + x_3)^2 + x_2 \tag{27}$$

where x_1 is stochastic variable following standard normal distribution, x_2 follows normal distribution of $\mathcal{N}(\mu, 2)$ with $\mu \in [-2, 1]$, and x_3 is the deterministic variable following uniform distribution of $x_3 \in [-1, 2]$. We perform CABO and BAL method to estimate the bounds of failure probability. Initially we set the number of sampling pool with the size of N_z as 10000, the number of training samples as 12, and the error tolerance of learning functions as 10^{-3}. The reference and the estimation results of $g_1(x)$ are displayed in Figure 2. and Table 1. As is shown in Table 1, evaluating the lower bound using BAL consumed only 45.34s, compared to the 438.88s required by CABO. This drastic reduction in computational time is achieved because BAL completely avoids the KL expansion used in CABO framework. CABO requires the spectral decomposition of a large covariance matrix to directly sample from the posterior GPR model, which becomes computationally prohibitive and impractical for the rare events. In contrast, the proposed BAL method utilizes pointwise UCB criteria to evaluate epistemic uncertain-ty independently at each candidate point, thereby bypassing the time-consuming KL expansion altogether. Consequently, the computational overhead is greatly reduced while successfully reaching the global optimal points as the convergence condition is satisfied, as evidenced by the convergence condition shown in Figure 3.

For g_2-function, we estimate the failure probability of rare events and set the initial number as is mentioned above. As can be seen in Table 2, estimating the lower bound of the failure probability required only 8 additional simulator calls for the BAL-SS. The SS methods is capable of estimating failure probability of rare events with limited sample size, whereas the MCS method fails to achieve comparable efficiency within the double-loop framework. The SS method fundamentally overcomes this limitation by systematically stratifying the aleatory space, ensuring that extreme tail regions are adequately represented without the need for brute-force massive sampling.

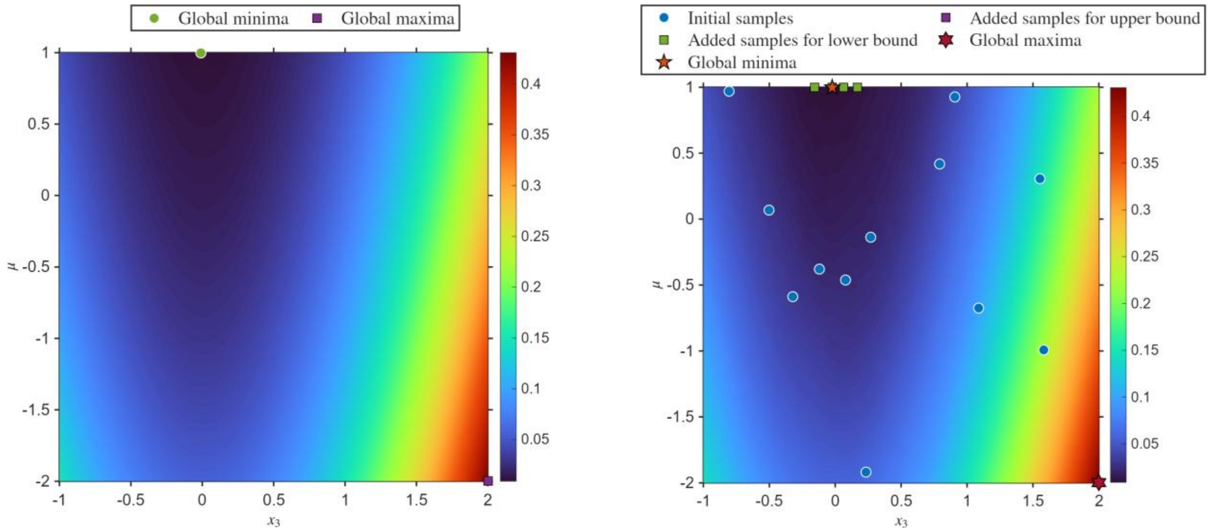

(a) The reference result of $g_1(x)$. (b) The estimation result of $g_1(x)$.

Figure 3. The training details of calculating design point of the bounds of three-dimensional case1.

Table I. Results of reliability analysis for g_1-function.

Method	*Sampling Method*	*Bounds*	P_f	*Optima of* $(x_{\mathrm{III}},\theta)$	*COV*	*Number of Calls*	*Time(s)*
CABO	*MCS*	Lower	0.0076	(-0.0420,1)	0.1601	12+4+9	428.88
		Upper	0.4322	(-2,2)	0.0114		169.39
BAL		Lower	0.0089	(-0.0353,1)	0.0052	12+8+4	45.23
		Upper	0.4322	(-2,2)	0.0041		115.48
Reference		Lower	0.0088	(-0.0264,1)	--	--	--
		Upper	0.4308	(-2,2)			

Table II. Results of reliability analysis for g_2-function.

Method	*Sampling Method*	*Bounds*	P_f	*Optima of* $(x_{\mathrm{III}},\theta)$	*COV*	*Number of Calls*
BAL	*MCS*	*Lower*	--	--	--	--
		Upper	0.0147	(2,-2)	0.0082	12+6
	SS	*Lower*	7.783×10^{-6}	(-0.0039,1)	0.0267	12+8+11
		Upper	0.0150	(2,-2)	0.0208	

The results reported in Table I and II indicate that the both bounds of failure probability are accurately estimated with BAL-SS as the values of bounds match well with different sampling methods and the posterior COVs are sufficiently small. It is evident that the posterior COVs of the lower bound is higher than that of the upper bound, that's because the lower bound of failure probability is significantly smaller than the upper bound and is influenced by the significant aleatory uncertainties of inputs which makes it hard to estimate accurately.

4.2. Operating State Analysis Of Satellite

We consider a more detailed and realistic example. As is shown in Figure 4, the model calibration consists of a 7146-DOF generic communication satellite FE model with 1191 nodes and 1262 elements. It is assumed that the Young's moduli of different components of the satellite are characterized by different uncertainty 447 models given in Table III. Let random variables $\boldsymbol{x}_{\mathrm{I}}=(E_1,E_2)$ obey log-normal distribution with means 5.8×10^8 and variance 2.9×10^7. The imprecise random variables $\boldsymbol{x}_{\mathrm{II}}=E_3$ satisfy log-normal distribution where means are interval variables of $[2.4,3.6]\times10^5$ and variance are also interval variables of $[0.45,0.9]\times10^5$, let $\theta=(\mu_E,\sigma_E)$. The interval random variables $\boldsymbol{x}_{\mathrm{III}}=(E_4,E_5)$ are suggested as uniform distribution of interval $[6.4,9.6]\times10^{10}$.

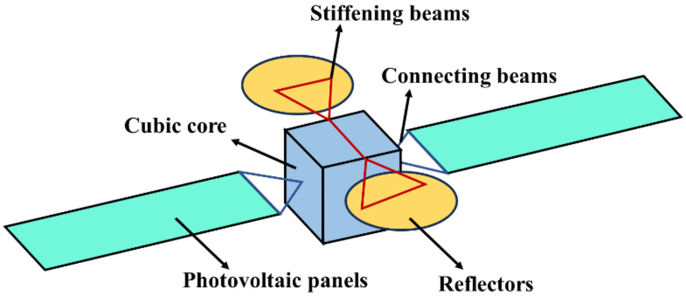

Figure 4. The structure of satellite.

In this structure of the satellite, the cubic core is fixed with reflectors and photovoltaic panels by the connecting beams and stiffening beams. It is important for the first natural frequency to ensure the safety of satellite. Based on the above assumption, we suppose that the satellite will fail if the first natural frequency is less than the given threshold. Therefore, the LSF of the first natural frequency is formulated as:

$$g(\boldsymbol{x})=d_A(\boldsymbol{x})-0.16 \tag{28}$$

Table III. Distribution information of Young's modulus of the satellite.

Parameters	*Distribution Type*	*Means*	*Std*	*Range*
E_1 *(cubic core,* Pa*)*	*Log-normal*	5.8×10^8	2.9×10^7	
E_2 *(photovoltaic panels,* Pa*)*	*Log-normal*	5.8×10^8	2.9×10^7	
E_3 *(reflectors,* Pa*)*	*Log-normal*	$\mu_{E_3}\in[2.4,3.6]\times10^5$	$\sigma_{E_3}\in[0.45,0.9]\times10^5$	
E_4 *(connecting beams,* Pa*)*	*Uniform*			$[6.4,9.6]\times10^{10}$
E_5 *(stiffening beams,* Pa*)*	*Uniform*			$[6.4,9.6]\times10^{10}$

To estimate the bounds of the failure probability, the initial number $Ntrain$ of training samples is set as 30, the number of subdomains for BAL-SS method is set as 7 and the number of samples in each subdomain is set as 1000. While the convergence criterion ε is defined as 10^{-2}, the parameters a and b are defined as 1 and 1.5 to speed up the convergence rate. The results shown in Table IV indicate that the estimations failure probability bounds are accurate and efficient because the COVs are less than 5% and the number of calls of the whole procedure is adequately small.

Table IV. Results of reliability analysis for satellite.

Method	*Bounds*	P_f	*Optima of* $(E_4, E_5, \mu_{E_3}, \sigma_{E_3})$	*COV*	*Number of Calls*
CABO	Lower	--	--	--	30+33
	Upper	0.4914	$(6.4000\times10^{10}, 6.4000\times10^{10})$ $(2.4000\times10^{5}, 0.9000\times10^{5})$	0.0051	
BAL-SS	Lower	6×10^{-4}	$(8.3120\times10^{10}, 8.7216\times10^{10})$ $(2.8251\times10^{5}, 0.4500\times10^{5})$	0.0408	30+43+18
	Upper	0.4914	$(6.4000\times10^{10}, 6.4000\times10^{10})$ $(2.4000\times10^{5}, 0.9000\times10^{5})$	0.0102	

5. Conclusions

This work presents a computationally efficient algorithm for reliability analysis called BAL-SS, to effectively estimate the bounds of small failure probability under hybrid aleatory and epistemic uncertainties. Before applying the procedure of BAL-SS, we characterize the input variables by three models respectively, which are precise probabilistic model, non-probabilistic model and imprecise probabilistic model. It is suggested to transform those input variables to independent uniform distributional inputs and interval epistemic parameters. Then we implement adaptive Bayesian optimization scheme to update the GPR model in the epistemic uncertainty space. Specifically, we develop a new learning function to propagate epistemic uncertainties especially non-parametric uncertainties caused by GPR model and search the optimal points in epistemic uncertainty space of failure probability boundary. U function is applied to produce optimal points in aleatory uncertainty space and infer the posterior distribution of failure probability at deterministic sites specified by PSO algorithm. The two learning functions generate a set of new training points to update the GPR model until the process of optimizing and updating is convergent. By integrate the proposed Bayesian active learning function with a stratified sampling method, the framework effectively overcomes the double-loop computational curse and the challenges associated with rare event.

Acknowledgements

This work is supported by the National Natural Science Foundation of China under grant number 52475164.

References

Beer M., Ferson S. and Kreinovich V. Imprecise probabilities in engineering analyses. *Mechanical Systems and Signal Processing* 37:4–29, 2013.

Crespo, L. G., Kenny, S. P., Giesy, D. P. Reliability Analysis of Polynomial Systems Subject to P-Box Uncertainties. *Mechanical System and Signal Processing*, 37:121–136, 2013.

Stein, M., Beer, M., Kreinovich, V. Bayesian Approach for Inconsistent Information. *Information Sciences*, 245:96–111, 2013.

Blair, A. N., Ayyub, B. M., Bender, W. J. Fuzzy Stochastic Risk-Based Decision Analysis with the Mobile Offshore Base as a Case Study. *Marine Structures*, 14:69–88, 2001.

Agarwal, H., Renaud, J. E., Preston, E. L., et al. Uncertainty Quantification Using Evidence Theory in Multidisciplinary Design Optimization. *Reliability Engineering & System Safety*, 85(1/3):281–294, 2004.

McGill, W. L., Ayyub, B. M. Estimating Parameter Distributions in Structural Reliability Assessment Using the Transferable Belief Model. *Computers & Structures*, 86(10–11):1052–1060, 2008.

Zhang, J. X., Shields, M. D. On the Quantification and Efficient Propagation of Imprecise Probabilities Resulting from Small Datasets. *Mechanical Systems and Signal Processing*, 98:465–483, 2018.

Zhang, H., Mullen, R. L., Muhanna, R. L. Interval Monte Carlo Methods for Structural Reliability. *Structural Safety*, 32(3):183–190, 2010.

Zhang, H., Dai, H., Beer, M., et al. Structural Reliability Analysis on the Basis of Small Samples: An Interval Quasi-Monte Carlo Method. *Mechanical Systems and Signal Processing*, 37(1–2):137–151, 2013.

Zhao, Z., Lu, Z. H., Zhao, Y. G., et al. A Novel Random-Interval Hybrid Reliability Analysis Method Combining Active Learning Kriging and Two-Phase Subset Simulation. *Structures*, 63:106383, 2024.

Zhang, H. Interval Importance Sampling Method for Finite Element-Based Structural Reliability Assessment Under Parameter Uncertainties. *Structural Safety*, 38:1–10, 2012.

Alvarez, D. A., Uribe, F., Hurtado, J. E. Estimation of the Lower and Upper Bounds on the Probability of Failure Using Subset Simulation and Random Set Theory. *Mechanical Systems and Signal Processing*, 100:782–801, 2018.

Wei, P. F., Lu, Z. Z. and Song, J. W. Extended Monte Carlo Simulation for Parametric Global Sensitivity Analysis and Optimization. *AIAA Journal*, 52:867-878, 2014.

Wei, P. F., Song, J. W., Bi, S. F., et al. Non-Intrusive Stochastic Analysis with Parameterized Imprecise Probability Models: I. Performance Estimation. *Mechanical Systems and Signal Processing*, 124:349-368, 2019.

Wei, P. F., Song, J. W., Bi, S. F., et al. Non-Intrusive Stochastic Analysis with Parameterized Imprecise Probability Models: II. Reliability and Rare Events Analysis. *Mechanical Systems and Signal Processing*, 126:227-247, 2019.

Song, J. W., Valdebenito, M., Wei, P. F., et al. Non-Intrusive Imprecise Stochastic Simulation by Line Sampling. *Structural Safety*, 84:101936, 2020.

Faes, M. G., Valdebenito, M. A., Moens, D., et al. Operator Norm Theory as an Efficient Tool to Propagate Hybrid Uncertainties and Calculate Imprecise Probabilities. *Mechanical Systems and Signal Processing*, 152:107482, 2021.

Hong, F. Q., Wei, P. F., Fu, J. F., et al. A Sequential Sampling-Based Bayesian Numerical Method for Reliability-Based Design Optimization. *Reliability Engineering & System Safety*, 244:109939, 2024.

Hong, F. Q., Wei, P. F., Song, J. W., et al. Collaborative and Adaptive Bayesian Optimization for Bounding Variances and Probabilities Under Hybrid Uncertainties. *Computer Methods in Applied Mechanics and Engineering*, 417:116410, 2023.

Wei, P. F., Hong, F. Q., Phoon, K. K., et al. Bounds Optimization of Model Response Moments: A Twin-Engine Bayesian Active Learning Method. *Computational Mechanics*, 67:1273-1292, 2021.

Li, C. C., Der Kiureghian, A. Optimal Discretization of Random Fields. *Journal of Engineering Mechanics*, 119(6):1136-1154, 1993.

Huang, S., Mahadevan, S., Rebba, R. Collocation-Based Stochastic Finite Element Analysis for Random Field Problems. *Probabilistic Engineering Mechanics*, 22(2):194-205, 2007.

Chen, J., Kong, F., Peng, Y. A Stochastic Harmonic Function Representation for Non-Stationary Stochastic Processes. *Mechanical Systems and Signal Processing*, 96:31-44, 2017.

Wilson, J., Borovitskiy, V., Terenin, A., et al. Efficiently Sampling Functions from Gaussian Process Posteriors. *International Conference on Machine Learning*. PMLR, 10292-10302, 2020.

Vakili, S., Moss, H., Artemev, A., et al. Scalable Thompson Sampling Using Sparse Gaussian Process Models. *Advances in Neural Information Processing Systems*, 34:5631-5643, 2021.

Echard, B., Gayton, N., Lemaire, M. AK-MCS: An Active Learning Reliability Method Combining Kriging and Monte Carlo Simulation. *Structural Safety*, 33(2):145-154, 2011.

Bichon, B. J., Eldred, M., Swiler, L. P., et al. Efficient Global Reliability Analysis for Nonlinear Implicit Performance Functions. *AIAA Journal*, 46:2459-2468, 2008.

Lv, Z. Y., Lu, Z. Z., Wang, P. A New Learning Function for Kriging and Its Applications to Solve Reliability Problems in Engineering. *Computers & Mathematics with Applications*, 70(5):1182-1197, 2015.